Journal of Applied Pharmaceutical Research
Volume 14 Issue 1, Year of Publication 2026, Page 66 – 75
DOI: https://doi.org/10.69857/joapr.v14i1.1517

Check for updates

Research Article

JOURNAL OF APPLIED PHARMACEUTICAL RESEARCH | JOAPR
www.japtronline.com ***ISSN: 2348 – 0335***

FORMULATION AND OPTIMIZATION OF SIMVASTATIN LOADED NANOSTRUCTURED LIPID CARRIERS USING CENTRAL COMPOSITE DESIGN

Subramanyam Nikhila, Chinthaginjala Haranath*, Dasari Bhargavi, Gogula Priya, Yaga Maheswar Reddy

Article Information
Received: 25th September 2025
Revised: 17th November 2025
Accepted: 13th December 2025
Published: 4th January 2026

Keywords
Entrapment efficiency, Nanostructured lipid carriers, Particle size, Simvastatin, Zeta potential

ABSTRACT
Background: This study aimed to formulate and optimize simvastatin-loaded nanostructured lipid carriers using central composite design. The concentrations of stearic acid, olive oil, and surfactant were designated as independent variables. The dependent variables nominated were particle size, zeta potential, and % entrapment efficiency. **Methodology:** Simvastatin-loaded nanostructured lipid carriers were prepared using the solvent-injection method. Polynomial equations were used to forecast the quantifiable impact of independent factors at various levels on response variables. It was found that the curvature effect was substantial and that the model was nonlinear. To optimize, the study employed the central composite design. **Results & Discussions:** Studies using DSC and FT-IR showed that the drug and excipients were compatible. The particle size, polydispersity index, and zeta potential values of all formulations were within the range of 133.8-460.7 nm, 0.215-0.460, and -28.3 to -32.1, respectively. The study's outcomes confirmed that olive oil significantly affects particle size and % entrapment efficiency. The relationships between the independent variables and the dependent variables were elucidated using contour plots. The experimental results and the model's predicted values were reasonably close; the statistical model can be considered mathematically valid. **Conclusion:** The outcomes confirmed the efficacy of the proposed design for developing simvastatin-loaded nanostructured lipid carriers with optimized properties.

INTRODUCTION

Nanotechnology is increasingly being used for drug delivery via multiple administration routes [1]. The solid lipid core of lipid nanocarriers, called Nanostructured lipid carriers (NLC), is made up of a combination of liquid and solid lipids [2]. Simvastatin (SIM) is a well-known drug that reduces the risk of heart attack, stroke, and other cardiac events by lowering blood levels of triglycerides (TG) and low-density lipoproteins (LDL) and increasing high-density lipoproteins (HDL) [3]. The main drawback of SIM is its low bioavailability (5%), more protein binding capacity (95%), and it is metabolized in the liver (CYP3A4) and has a relatively short biological half-life of two

**Department of Pharmaceutics, Raghavendra Institute of Pharmaceutical Education and Research (RIPER)- Autonomous, KR palli cross, Chiyyedu post, Ananthapuramu, 515721, Andhra Pradesh, India*

For Correspondence: **haranathriper@gmail.com**

hours [4]. Therefore, to achieve the desired effect, a higher dose of the drug is required, which may lead to more severe adverse reactions in the muscles & liver [5]. Formulating drugs as nanocarriers can improve bioavailability and biological activity while reducing drug toxicity [6]. NLC can enhance drug loading capacity, prevent early drug release and leakage, and increase permeation efficiency [7]. A novel idea for the development of high-quality pharmaceutical goods is called Quality by Design (QbD) [8]. Central composite design (CCD) is a statistical technique used for formulation optimization. To create a design space for regulatory flexibility, the CCD tool [9] was used to assess input and output variables systematically. The current study aims to evaluate the use of CCD to develop NLCs of SIM & to investigate the effects of factors on the responses. The concentration of stearic acid, olive oil, and surfactant was designated as an independent variable. The dependent variables selected were particle size (PS), zeta potential (ZP), and % entrapment efficiency (EE).

MATERIALS AND METHODS

Materials: SIM was supplied as a gift sample by Microlabs, Bengaluru. Stearic acid, Olive oil, Pluronic F68 & acetone were acquired from Loba Chemie, Mumbai. All elements used were of analytical grade.

Table 1: Input factors with responses

Factors	Actual values					Response
	-2	-1	0	+1	+2	
Stearic acid	50	100	150	200	250	Y1- Particle size, Y2 - Zeta potential, Y3-Entrapment efficiency
Olive oil	7.5	15	22.5	30	37.5	
Pluronic F68	0.5	0.75	1	1.25	1.5	

Table 2: Formulation design

	Code	Combinations	X_1(SA)	X_2(OO)	X_3(PF68)
Factorial Design	F_1	I	100	15	0.75
	F_2	X_1	200	15	0.75
	F_3	X_2	100	30	0.75
	F_4	X_1 X_2	200	30	0.75
	F_5	X_3	100	15	1.25
	F_6	X_1 X_3	200	15	1.25
	F_7	X_2 X_3	100	30	1.25
	F_8	X_1 X_2 X_3	200	30	1.25
Mid point	F_9	Mid point	150	22.5	1.0
Central Composite Design	F_{10}	X_1 At -2L	50	22.5	1.0
	F_{11}	X_1 At +2L	250	22.5	1.0
	F_{12}	X_2 At -2L	150	7.5	1.0
	F_{13}	X_2 At +2L	150	37.5	1.0
	F_{14}	X_3 At -2L	150	22.5	0.5
	F_{15}	X_3 At +2L	150	22.5	1.5

Table 3: Composition of SIM-NLCs (F_1- F_8)

Ingredients	F_1	F_2	F_3	F_4	F_5	F_6	F_7	F_8
SIM(mg)	15	15	15	15	15	15	15	15
SA (mg)	100	200	100	200	100	200	100	200
Olive oil (ml)	1.85	1.85	3.70	3.70	1.85	1.85	3.70	3.70
Acetone (ml)	2	2	2	2	2	2	2	2
Pluronic F68 (mg)	150	150	150	150	250	250	250	250
Water (ml)	20	20	20	20	20	20	20	20

Table 4: Composition of SIM-NLCs (F_9- F_{15})

Ingredients	F_9	F_{10}	F_{11}	F_{12}	F_{13}	F_{14}	F_{15}
SIM (mg)	15	15	15	15	15	15	15
SA (mg)	150	50	250	150	150	150	150
Olive oil (ml)	2.775	2.775	2.775	0.925	4.62	2.77	2.775
Acetone (ml)	2	2	2	2	2	2	2
Pluronic F68 (mg)	150	150	150	150	250	250	250
Water (ml)	20	20	20	20	20	20	20

FT-IR studies: FT-IR spectra for pure SIM and their physical mixtures were obtained employing the potassium bromide (KBr) pellet technique. In this method, the samples were blended with dry, IR-grade crystalline KBr and then compressed at 10 tons using a hydraulic press to produce thin disks [10]. The resulting spectra were collected within the 400–4000 cm^{-1} range on an FTIR (Bruker Alpha T).

Thermal analysis: Pure SIM powder and a physical mixture were investigated using a differential scanning calorimeter (DSC, Venchal Scientific model 412105). An appropriate quantity of sample (5 mg) was placed into a sealed aluminum pan and heated from 50°C to 300°C at a rate of 10°C per minute. An empty aluminum pan was used as a reference during the analysis [11]

Optimization by the CCD: In the current study, a CCD, including factorial, axial, and center points, was used to optimize NLCs. Independent variables were selected as Conc. of Stearic acid (SA) (X_1), conc. of Olive oil (OO) (X_2) and conc. of Poloxamer F68 (X_3). All were set at low and high levels. Responses were preferred PS, ZP & EE. The actual and coded values of the variables are presented in Table 1. According to the design, formulations of SIM-NLCs were developed & represented in Table 2.

Method of preparation of SIM-NLCs

SIM-NLCs were prepared by the Solvent Injection method. In 2 ml of acetone, 15 mg of SIM and specified quantities of SA and OO were dissolved as given in Table 3 and Table 4 with heating at the melting point of SA (at 69.3°C).

The resulting solution was rapidly injected into 20 ml of aqueous solution containing a specified amount of Pluronic F68, which was continuously stirred on a magnetic stirrer at 400 rpm for 30 min. 4 ml of 0.1 N HCl was then added to the mixture to facilitate separation by inducing NLC aggregation. Afterwards, the solution was centrifuged for 30 mins at 5,000 rpm [12].

CHARACTERIZATION

PS, PDI, and ZP

The average PS, PDI, and ZP were measured by a Nanoparticle size analyzer (Horiba). The prepared samples were properly diluted with deionized, double-distilled water to avoid multiple scattering [13]. The diluted samples were kept in cuvettes, and all measurements were performed at 25 ± 0.5 °C. The ZP of dispersion should be < -30 mV or > + 30 mV, which indicates the electrostatic stability [14].

%EE

The % EE of SIM-NLCs was determined by using an indirect technique. An appropriate volume of the sample was centrifuged at 3000 rpm for 30 min [15]. Thus, the obtained supernatant was appropriately diluted, and the amount of free drug was measured using a UV spectrophotometer at λmax = 239 nm against the diluted supernatant of the blank NLC solution. The actual amount of SIM was calculated by spectrophotometrically dissolving nanoparticles in methanol.

$$\% \, \boldsymbol{EE} = \frac{\boldsymbol{W\ total - W\ free}}{\boldsymbol{W\ total}} \times \mathbf{100}$$

W total = actual amount of SIM added; W free = amount of SIM sensed in the supernatant

In vitro drug release (IVDR)

Using the dialysis bag diffusion technique, IVDR was performed [16]. The dialysis bag was filled with NLCs of SIM and submerged in a 100 mL compartment of 7.4 pH phosphate buffer, which was stirred at 100 rpm at 37 ± 0.5 °C. At intervals of up to 24 hours, 5 mL aliquots were removed and replaced with an appropriately diluted volume of dissolving medium. The concentration was then determined using UV-Visible spectrophotometry at a wavelength of 239 nm.

Statistical analysis

To develop the experimental design, the statistics for all formulations were evaluated using Sigma Tech software. An assessment of several statistical limitations identified the best-fit model. To identify significant variable features on response regression coefficients, an ANOVA was used [17]. Using contour designs, the relationship between dependent and independent variables was examined. Exclusive experiments with the expected results were developed using a graphic optimization method with CP. PS, ZP, and EE were assessed to ensure they aligned with the hypothetical estimate. The RE between the observed and anticipated results was estimated for each response.

RESULTS AND DISCUSSION

Results

FT-IR & DSC Studies

FTIR & DSC studies were performed on the pure drug and the excipients to confirm compatibility with all excipients, as shown in Figures 1 and 2.

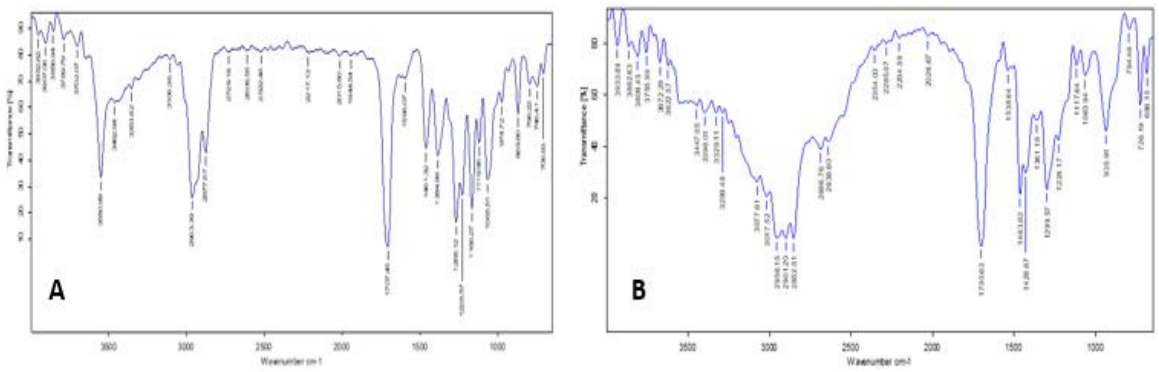

Figure 1: A) FT-IR spectra of SIM B) FT-IR spectra of blend

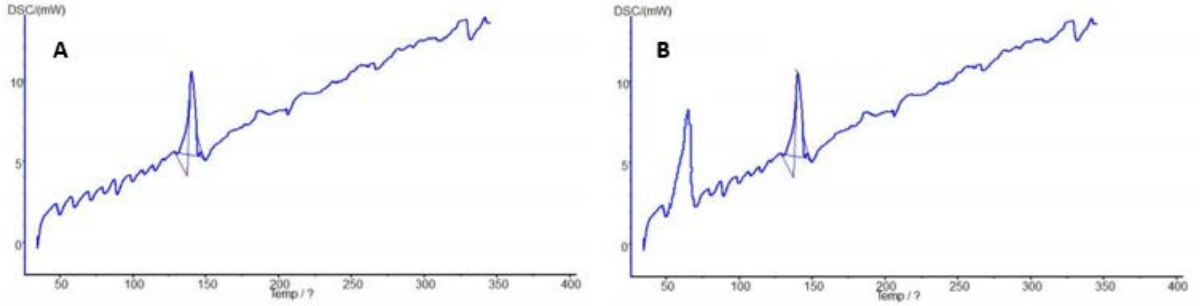

Figure 2: A) DSC thermograms of SIM B) DSC thermogram of blend

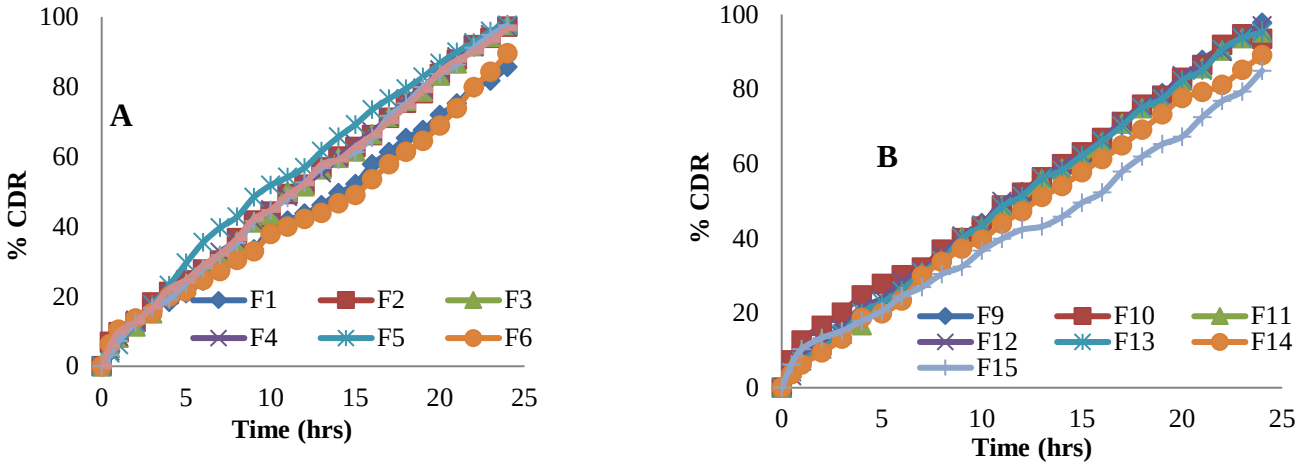

Figure 3: A) IVDR outline of F1-F8, B) IVDR outline of F9 – F15

Table 6: Outcomes of ANOVA for Y_1 (PS)

S. No	Source of variable	SS	DF	MS	F-value	F std at 0.1p	F std at 0.05p	F std at 0.01p
1	Model	6.8615	6	1.1435	10.1	3.9	4.5	8.6
2	Error	0.0	1	0.0				
3	Total	6.8615	7					
95% confident level of curvature effect -Non-linear								

SD: 0.04; CE: -22.836; F SV at 0.05 p:10.9; F SV at 0.01 p : 32.8; 95% CLCE: FROM -24.475 TO: -22.285

Table 7: Outcomes of ANOVA for Y_2 (ZP)

S.No	Source of variable	SS	DF	MS	F-value	F std at 0.1p	F std at 0.05p	F std at 0.01p
1	Model	11.1558	4	1.8592	11.5	4.6	5.8	9.7
2	Error	0.0	1	0.0				
3	Total	11.1558	5					
95% confident level of curvature effect- Non-linear								

SD: 0.05; CE: -9.26; F SV at 0.05 p: 12.4; F SV at 0.01 p: 30.7; 95% CLCE: FROM -11.85 TO -9.94

Table 8: Outcomes of ANOVA for Y_3 (% EE)

S.No	Source of variable	SS	DF	MS	F-value	F std at 0.1p	F std at 0.05p	F std at 0.01p
1	Model	12.1567	5	2.0261	9.6	3.6	5.3	8.5
2	Error	0	1	0				
3	Total	12.1567	6					

SD: 0.08; CE: -11.65; F SV at 0.05 p: 10.1; F SV at 0.01 p: 34.1; 95% CLCE: FROM -13.12 TO -11.82

Experimental values and predicted values: The results **of** experimental values and predicted values were tabulated in Table 9.

Table 9: Comparison of experimental results with predicted responses.

Ingredients	Composition	Response	Predicted value	Experiment Value
SA	100 mg	Y1 (Particle Size)	250 nm	251.3 nm
OO	1.85 ml	Y2 (Zeta Potential)	-30 mV	-29.5 mV
PLU	250 mg	Y3 (% Entrapment Efficiency)	98 %	97.67%

Contour Plots: The contour plots of PS, ZP, and EE were presented in Figures 4, 5, and 6, respectively.

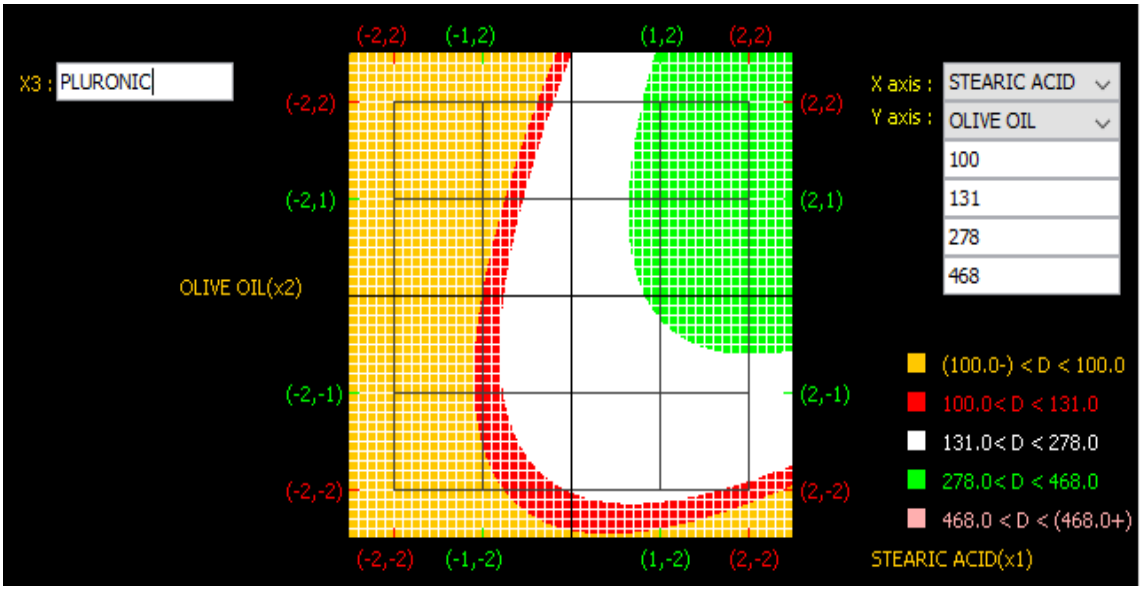

Figure 4: Contour plot of PS

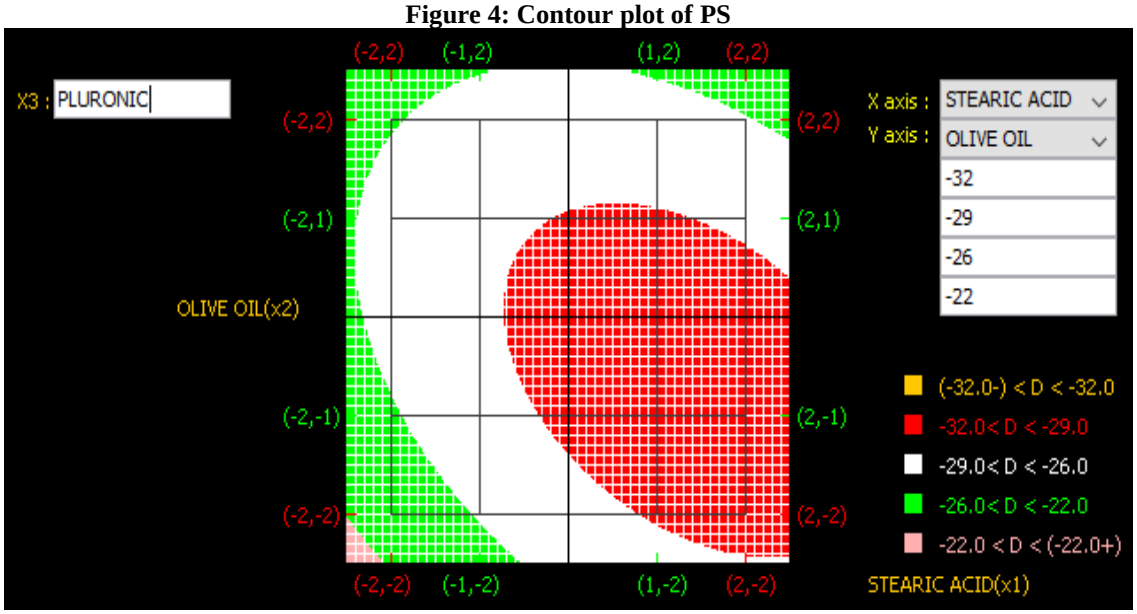

Figure 5: Contour plot of ZP

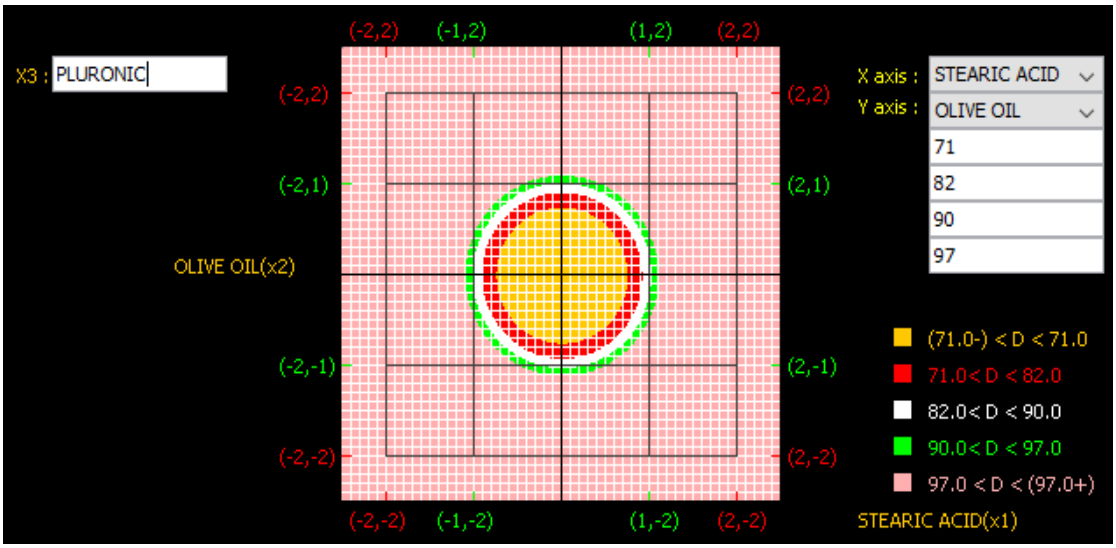

Figure 6: Contour plot of EE

DISCUSSION

FT-IR and DSC Studies

Using FT-IR and DSC, drug–excipient compatibility was evaluated. The presence of any likely interactions between the drug and the physical mixture was scanned over the range 4000–400 cm^{-1}. Figure 1 demonstrates the FT-IR spectra of SIM and the blend, respectively. SIM exhibited characteristic peaks at 3462 (O-H, Phenol), 2963 (C-H), 1707 (C=O), 1596 (C=C), and 1268 cm−1 (C-O). The physical mixture shows peaks at 3447 (O-H Phenol), 2956 (C-H), 1700 (C=O), 1538 (C=C), and 1299 cm^{-1} (C-O). It also implies that the drug and its chemical interactions do not exist with other ingredients [18]. There are no major shifts in the peaks of the drug and excipients used in the formulation. DSC analysis was executed for the drug and physical mixture [19]. As shown in Figure 2, the drug shows a sharp endothermic peak at 140°C, signifying the melting nature of the drug. The physical mixture also retained the peaks. The drug and excipient peaks in the formulation show no significant changes, as indicated by DSC analysis.

PS: The PS of the SIM-NLCs formulations (F1-F15) ranged from 133.8 nm to 460.7 nm, as shown in Table 5. Analysis of the PS data revealed that the interaction among factors X1, X2, and X3 contributed the most (37.7%) and had a positive coefficient (72.025), indicating that increasing the levels of these variables increased PS. ANOVA showed a significant effect, with a high coefficient of determination (R^2 = 0.9929). The calculated F-value (10.1) exceeded the critical value (4.5), indicating statistical significance at $p < 0.05$, as detailed in Table 6. Given the significant R^2, this model is appropriate for predictive purposes. Furthermore, the nonlinear relationship between Y1 and the interaction term X1X2X3, identified using Sigma Tech, justified the use of the Central Composite Design (CCD). Using Sigma Tech, a quadratic statistical model was fitted to the data.

Final equation in terms of coded factors

$$Y1 = 33.0111 + 5.475\,X1 + 4.785\,X2 + 1.6138\,X3 + 2.885\,X1X2 - 0.3325\,X1X3 - 2.22225\,X2X3 + 28.3686\,X1^2 + 30.5061\,X2^2 + 26.6436\,X3^2$$

Final equation in terms of actual factors

$$PS = 33.0111 + 5.475\,SA + 4.785\,OO + 1.6138\,PLU + 2.885\,SA.OO - 0.3325\,SA.PLU - 2.22225\,OO.PLU + 28.3686SA^2 + 30.5061\,OO^2 + 26.6436\,PLU^2$$

The multinomial equation was used to draw inferences by considering the magnitude of the coefficient and its sign (i.e., negative or positive). The results of multiple linear regression analysis revealed that PS decreased with increasing olive oil concentration, whereas stearic acid and pluronic F68 concentrations decreased. Olive oil (OO) is recognized as a key contributor to particle size reduction [20]. Increasing the proportion of liquid lipid reduces particle size. Conversely, a rise in liquid lipid content can also result in larger particle sizes, which may be explained by the higher entrapment efficiency (EE) observed with increased liquid lipid levels. In nanostructured lipid carriers (NLCs), where the liquid lipid forms the core encased in solid lipid, a greater total lipid amount can cause the particles to become larger. At low to moderate concentrations, increasing the amount of olive oil (a liquid lipid)

generally reduces particle size. This occurs because liquid lipids reduce the viscosity of the internal phase and increase the mobility of surfactant molecules at the interface, thereby promoting the formation of smaller particles during homogenization or sonication.

Additionally, a higher proportion of liquid lipid often reduces the ordering and crystallinity of the solid matrix, thereby facilitating the formation of smaller, more uniformly distributed nanoparticles. However, beyond a certain threshold, further increases in liquid lipid concentration may increase particle size. This effect is attributed to particle coalescence and an increase in the volume of the dispersed (lipid) phase, resulting in larger droplets before solidification. A higher liquid lipid content increases the surface area to be stabilized, potentially overwhelming the surfactant's stabilizing capacity and ultimately causing droplets to merge or grow larger. At low stabilizer concentrations, insufficient stabilizer may fail to inhibit particle growth, whereas excess stabilizer at high concentrations can coat particles and increase particle size. The R^2 value for the quadratic model was 0.9929, exceeding the threshold of 0.7, indicating strong model fit.

Poly Dispersity Index (PDI)

PDI is a dimensionless metric that quantifies the breadth of a particle-size distribution. It ranges from 0 to 1; values above 0.5 indicate a broad, heterogeneous particle distribution, typically associated with instability and non-uniformity in the formulation. Therefore, formulations exhibiting PDI values greater than 0.5 are generally unfavorable. In the case of SIM-NLCs formulations (F1-F15), the PDI values ranged from 0.215 to 0.462. Olive oil (OO) significantly reduces both PS and PDI by decreasing viscosity and surface tension in the NLC system, thereby promoting the formation of uniformly sized nanoparticles [21]. Additionally, increased lipid content may enhance drug loading capacity, resulting in larger particle sizes and greater variability in size distribution.

Zeta Potential (ZP)

The ZP of the SIM-NLCs formulations (F1-F15) ranged from -32.1 mV to -28.3 mV, as reported in Table 5, indicating thermodynamic stability. Analysis of the ZP data revealed that factor X1 had the most pronounced effect, accounting for 80.67% of the variance with a negative coefficient of -0.1875. In NLCs, the solid lipid matrix forms the outer shell around the liquid lipid core, positioning more ionizable groups outward as SA increases, which amplifies charge density without excessive particle growth. Stearic acid is a long-chain fatty acid that can ionize at the particle–water interface, exposing deprotonated carboxylate groups in aqueous medium.

As its concentration in the lipid matrix increases, a higher density of ionizable groups is present at the droplet surface, shifting the slipping-plane potential toward more negative values and thereby lowering the measured zeta potential. The negative coefficient of stearic acid in the polynomial equation for zeta potential indicates that increasing stearic acid concentration makes the surface charge more negative. This increase in negative surface charge typically corresponds to greater electrostatic repulsion between particles, thereby improving the physical stability of the dispersion by preventing aggregation. ANOVA was performed to assess the significance of these effects [22]. The coefficient of determination (R^2) was 0.784, indicating a reasonably good fit. Moreover, the calculated F-value of 11.5 exceeded the critical F-value of 5.8, confirming statistical significance at $p<0.05$ (Table 7). Therefore, it can be inferred that the observed F-value is unlikely to be due to random chance and signifies a meaningful effect at the specified significance level.

Final equation in terms of coded factors

$$Y2 = 170.4222 – 0.1875\,X1 + 0.59\,X2 – 0.4362\,X3 + 2.885\,X1X2 - 0.3325\,X1X3 - 2.22225\,X2X3 – 40.2453\,X1^2 – 40.0953\,X2^2 – 40.2578\,X3^2$$

Final equation in terms of actual factors

$$ZP = 170.4222 – 0.1875\,SA + 0.59\,OO – 0.4362\,PLU + 2.885\,SA.OO - 0.3325\,SA.PLU - 2.22225\,OO.PLU – 40.2453\,SA^2 – 40.0953\,OO^2 – 40.2578\,PLU^2$$

The multiple linear regression analysis showed that the zeta potential declined as the concentrations of stearic acid and pluronic F68 increased. The quadratic model had a coefficient of determination (R^2) of 0.784, exceeding the 0.7 threshold, indicating a good fit.

% Entrapment Efficiency (%EE)

The % EE of the SIM-NLC formulations (F1–F15) ranged from 83.39% to 94.95%. After EE data analysis, the interaction between X1 and X2, with a positive coefficient (2.885), was found to be the largest (41.094%). It showed that EE increased with increasing quantities of X1 and X2 (Table 8).

Final equation in terms of coded factors

$$Y3 = 92.1278+0.0675\ X1+1.4475\ X2-0.06\ X3+2.885\ X1X2-0.3325\ X1X3-2.22225\ X2X3-0.8735\ X1^2\ -1.0435\ X2^2\ -1.2397\ X3^2$$

Final equation in terms of actual factors

$$\%\ EE = 92.1278 + 0.0675\ SA + 1.4475\ OO - 0.06\ PLU + 2.885\ SA.OO - 0.3325\ SA.PLU - 2.22225\ OO.PLU - 0.8735\ SA^2 - 1.0435\ OO^2 - 1.2397\ PLU^2$$

The multiple linear regression analysis indicated that entrapment efficiency increased with higher concentrations of stearic acid and olive oil, whereas it decreased with increasing levels of pluronic F68 [23]. The quadratic model had a coefficient of determination (R^2) of 0.974, well above the 0.7 threshold, indicating strong model reliability.

IVDR

SIM-NLC formulations (F1-F15) showed in vitro percent drug release of 84.92%- 97.67% at the end of 24 hr (Figure 3).

Particle size and entrapment efficiency both influence drug release from nanocarrier systems, leading to expected variations in IVDR profiles across formulations. Consequently, formulation F5, with its relatively small particle size of 269.3 nm and high entrapment efficiency, exhibited the highest cumulative drug release in a controlled manner. The F5 formulation, with a moderate particle size and very high EE, appears optimal for sustained release. The moderately small size ensures a large surface area for drug diffusion. At the same time, the high EE indicates that a large fraction of the dose is molecularly dispersed or solubilized within the disordered lipid matrix rather than crystallized, supporting continuous release rather than a single burst. Formulations with very small sizes but lower EE tend to deplete their releasable drug earlier or exhibit less controlled profiles. In contrast, larger, highly loaded systems may show slower or incomplete release within 24 h.

In contrast, F5 balances these parameters so that drug molecules located in the defect-rich lipid network can gradually partition into the external buffer, resulting in near-complete but sustained release over the 24 h test period. OO had a major impact on the percent CDR-time profile. Thus, at the optimal level of OO, particle size is reduced, leading to an increased specific surface area and, consequently, a higher % CDR [24]. The relative proportion of liquid lipid (olive oil) in F5, in combination with solid lipid (stearic acid), creates a typical NLC-type imperfect crystalline matrix with multiple lattice defects. These structural imperfections increase the number of accommodation sites for simvastatin and decrease crystallinity, thereby enhancing molecular mobility and facilitating sustained diffusion of the drug through the lipid phase into the external medium over 24 h.

For F5, the presence of olive oil disrupts the ordering of stearic acid crystals, generating a less ordered β′/amorphous-like lipid structure typical of NLCs, which supports diffusion-controlled release. Simvastatin molecules are likely distributed in both the solid–liquid interfacial regions and within the liquid lipid-rich zones, from which they can diffuse progressively through the lipid and then across the dialysis membrane into the medium. Additionally, the higher surfactant level around F5 particles improves wettability and medium penetration into the lipid core, shortening the diffusion path length in the aqueous channels and helping to maintain sink conditions at the particle surface. One important factor to consider is the crystalline structure of the lipid matrix. In nanostructured lipid carriers (NLCs), combining solid and liquid lipids introduces defects and imperfections in the crystal lattice, resulting in a less-ordered structure. This can enhance drug mobility and release, as drug molecules are more readily able to diffuse through these imperfections.

The addition of olive oil (a liquid lipid) is known to promote such structural disorder, increasing the number of "imperfections" in solid lipid and ultimately facilitating higher drug release rates, independent of particle size. The elevated concentration of Pluronic F68 in F5 stabilizes the particles and prevents aggregation, maintaining a high effective surface area available for dissolution and diffusion. At this surfactant level, the surface is sufficiently covered to maintain dispersion stability without forming an excessively thick barrier. Surfactant concentration further influences drug release by stabilizing the nanoparticle surface and potentially affecting drug diffusion rates. Higher surfactant concentrations can improve dispersion and prevent aggregation, but excess surfactant may form micellar structures or thick films, thereby altering diffusion pathways. This complexity necessitates an optimal surfactant range for effective release. Lower surfactant concentrations may lead to incomplete stabilization, thereby affecting drug release, whereas very high concentrations may create barriers to drug diffusion from the carrier matrix. Figure 4 illustrates how contour plots were used to identify an appropriate design space for PS, ZP, and EE within the inferred values. The experimental

values were in agreement with the predicted values, confirming the model's predictability and validity, as shown in Table 9.

CONCLSION

The present study successfully formulated and statistically optimized simvastatin-loaded nanostructured lipid carriers (NLCs) using a central composite design approach. The model derived from experimental data effectively established the quantitative relationships between critical formulation variables—stearic acid, olive oil, and Pluronic F68 concentrations—and key responses including particle size, zeta potential, and entrapment efficiency. Using the desirability function, an optimal design space was identified and graphically represented, indicating the combination of formulation variables predicted to yield optimal performance characteristics. The optimized NLC formulation, developed using model-based desirability criteria and confirmed experimentally, exhibited a nanometric particle size, an optimal zeta potential for physical stability, high entrapment efficiency, and sustained drug release for up to 24 hours. The close agreement between predicted and observed responses validated the reliability of the optimization model. Hence, this study not only demonstrated the successful formulation of simvastatin NLCs but also completed the statistical optimization process, confirming that model-guided optimization and experimental validation can together ensure reproducible quality and performance of lipid-based nanocarriers for poorly soluble drugs such as simvastatin.

FINANCIAL ASSISTANCE

NIL

CONFLICT OF INTEREST

The authors declare no conflict of interest.

AUTHOR CONTRIBUTION

Subramanyam Nikhila conceptualized and designed the study**.** Dasari Bhargavi conducted the experimental work. Chinthaginjala Haranath provided supervision and expert guidance throughout the study. Gogula Priya conducted preformulation studies. Yaga Maheswar Reddy performed evaluation studies. All authors were equally involved in manuscript preparation and read and approved the final version.

REFERENCES

[1] Akbari J, Saeedi M, Ahmadi F, Hashemi SM, Babaei A, Yaddollahi S, Rostamkalaei SS, Asare-Addo K, Nokhodchi A. Solid lipid nanoparticles and nanostructured lipid carriers: A review of the methods of manufacture and routes of administration. *Pharm Dev Technol.*, **27**, 525-44 (2022) https://doi.org/10.1080/10837450.2022.2084554.

[2] Chinthaginjala H, Bogavalli V, Hindustan AA, Pathakamuri J, Pullaganti SS, Gowni A, Baktha B. Nanostructured lipid carriers: a potential era of drug delivery systems. *Ind. J. Pharm. Edu. Res.*, **58**, 21-33 (2024) https://doi.org/10.5530/ijper.58.1.3.

[3] Vuu YM, Kadar Shahib A, Rastegar M. The potential therapeutic application of simvastatin for brain complications and mechanisms of action. *Pharmaceuticals*., **16**, 914 (2023) https://doi.org/10.3390/ph16070914.

[4] Abd-Elghany AE, El-Garhy O, Fatease AA, Alamri AH, Abdelkader H. Enhancing oral bioavailability of simvastatin using uncoated and polymer-coated solid lipid nanoparticles. *Pharmaceutics*., **16**, 763(2024) https://doi.org/10.3390/pharmaceutics16060763.

[5] [5] Li JJ, Liu HH, Wu NQ, Yeo KK, Tan K, Ako J, Krittayaphong R, Tan RS, Aylward PE, Baek SH, Dalal J. Statin intolerance: an updated, narrative review mainly focusing on muscle adverse effects. *Expert Opin Drug Metab Toxicol.*, **16**, 837-51 (2020) https://doi.org/10.1080/17425255.2020.1802426.

[6] Malviya V, Pande S. A Review of the Most Recent Research on Solid Lipid Nanoparticles, Focusing on Active Compound Encapsulation. *Res J Pharm Technol.*, **18**, 1658-62 (2025) https://doi.org/10.52711/0974-360x.2025.00237.

[7] Sabale V, Jiwankar M. Nanostructured lipid carriers: An approach to oral delivery of drugs. *Res J Pharm Technol.*, **17**, 2427-30 (2024) https://doi.org/10.52711/0974-360x.2024.00380.

[8] Lee SH, Kim JK, Jee JP, Jang DJ, Park YJ, Kim JE. Quality by Design (QbD) application for the pharmaceutical development process. *J Pharm Investig.*, **5**, 649-82 (2022) https://doi.org/10.1007/s40005-022-00575-x

[9] Chinthaginjala H, Ahad HA, Srinivasa SK, Yaparla SR, Buddadasari S, Hassan JA, Pullaganti SS. Central composite design assisted formulation development and optimization of Gastroretentive floating tablets of dextromethorphan Hydrobromide. *Ind J Pharm Edu Res.*, **57**, 983-92 (2023) https://doi.org/10.5530/ijper.57.4.120.

[10] Markova E, Taneska L, Kostovska M, Shalabalija D, Mihailova L, Glavas Dodov M, Makreski P, Geskovski N, Petrushevska M, N. Taravari A, Simonoska Crcarevska M. Design and evaluation of nanostructured lipid carriers loaded with Salvia officinalis extract for Alzheimer's disease treatment. *J Biomed Mater Res B Appl Biomater*., **110,** 1368-90(2022) https://doi.org/10.1002/jbm.b.35006.

[11] Chinthaginjala H, Telkar MB, Hindustan AA, Bhupalam P. Formulation development and optimization of famotidine mucoadhesive tablets by central composite design. *Indian J. Pharm. Educ.*, **156**, (2022) https://doi.org/10.5530/ijper.56.4.185.

[12] Duong VA, Nguyen TT, Maeng HJ. Preparation of solid lipid nanoparticles and nanostructured lipid carriers for drug delivery and the effects of preparation parameters of solvent injection method. *Molecules.*, **25**, 4781 (2020) https://doi.org/10.3390/molecules25204781.

[13] Osanlou R, Emtyazjoo M, Banaei A, Hesarinejad MA, Ashrafi F. Preparation of solid lipid nanoparticles and nanostructured lipid carriers containing zeaxanthin and evaluation of physicochemical properties. *Colloids Surf A Physicochem Eng Asp.*, **641**, 128588 (2022) https://doi.org/10.1016/j.colsurfa.2022.128588.

[14] Houacine C, Adams D, Singh KK. Impact of liquid lipid on development and stability of trimyristin nanostructured lipid carriers for oral delivery of resveratrol. *J Mol Liq.*, **316**, 113734 (2020) https://doi.org/10.1016/j.molliq.2020.113734.

[15] Suyuti A, Hendradi E, Purwanti T. Physicochemical characteristics, entrapment efficiency, and stability of nanostructured lipid carriers loaded coenzyme Q10 with different lipid ratios. *J Res Pharm*., **27**, 1134-42(2023) https://doi.org/10.29228/jrp.404.

[16] Darwish MK, El-Enin AS, Mohammed KH. Optimized nanoparticles for enhanced oral bioavailability of a poorly soluble drug: solid lipid nanoparticles versus nanostructured lipid carriers. *Pharm Nanotechnol.*, **10**, 69-87 (2022) https://doi.org/10.2174/2211738510666220210110003.

[17] Naganaidu D, Khalid ZM. ANOVA assisted variable selection in high-dimensional multicategory response data. *Statistics.*, **11**, 92-100 (2023) https://doi.org/10.13189/ms.2023.110110.

[18] Ledeți I, Vlase G, Vlase T, Șuta LM, Todea A, Fuliaș A. Selection of solid-state excipients for simvastatin dosage forms through thermal and nonthermal techniques. *J Therm Anal Calorim.*, **121**, 1093-102 (2015) https://doi.org/10.1007/s10973-015-4832-5.

[19] Katkade PN, Zalte AG, Gondkar SB, Darekar AB, Amrutkar SV. Formulation, optimization, characterization and evaluation of Simvastatin loaded solid lipid nanoparticles using quality by design approach. *Res J Pharm Technol.*, **16**, 5872-7 (2023) https://doi.org/10.52711/0974-360x.2023.00951.

[20] Elsewedy HS, Shehata TM, Almostafa MM, Soliman WE. Hypolipidemic activity of olive oil-based nanostructured lipid carrier containing atorvastatin. *Nanomaterials.*, **12**, 2160 (2022) https://doi.org/10.3390/nano12132160.

[21] Subroto E, Andoyo R, Indiarto R. Solid lipid nanoparticles: review of the current research on encapsulation and delivery systems for active and antioxidant compounds. *Antioxidants.*, **12**, 633 (2023) https://doi.org/10.3390/antiox12030633.

[22] Aryani NL, Siswandono S, Soeratri W, Sari DR. Experimental development and molecular docking: nanostructured lipid carriers (NLCs) of coenzyme Q10 using stearic acid and different liquid lipids as lipid matrix. *Int J App Pharm.*, **13**, 108-16 (2021) https://doi.org/10.22159/ijap.2021v13i1.39890.

[23] Huguet-Casquero A, Moreno-Sastre M, López-Méndez TB, Gainza E, Pedraz JL. Encapsulation of oleuropein in nanostructured lipid carriers: Biocompatibility and antioxidant efficacy in lung epithelial cells. *Pharmaceutics.*, **12**, 429 (2020) https://doi.org/10.3390/pharmaceutics12050429.

[24] D'Souza A, Shegokar R. Nanostructured lipid carriers (NLCs) for drug delivery: Role of liquid lipid (oil). *Curr Drug Deliv.*, **18**, 249-70 (2021) https://doi.org/10.2174/1567201817666200423083807.